1969AcA....19....1P

ACTA ASTRONOMICA
Vol. 19, 1 1969

Envelopes of Red Supergiants

by

B. Paczyński

ABSTRACT

The detailed description of the computer programme used to calculate the model stellar envelopes with extended atmospheres is given. A large number of model envelopes of red supergiants was constructed with that programme. It is found that the inclusion of the opacity due to the H_2O molecules results in a decrease of the logarithm of the effective temperatures of the reddest model supergiants by 0·15. The effective temperatures slightly lower than 2000°K are consistent with the internal structure of those stars. The convection usually appears in the atmosphere but is not important for optical depth below 30. The red supergiants with $1\,\mathfrak{M}_\odot$ and $L > 2000\,L_\odot$ have the total energy of their envelopes positive when the recombination energy of the ionized hydrogen and helium is taken into account.

1. Introduction

The aim of this paper is to present a fairly detailed description of the computer programme used in Warsaw for the integrations of the equations of structure of stellar envelopes, including a simple gray atmosphere model. The programme is capable to handle the envelopes with extended atmospheres, and treats the convection within the mixing length formalism. It was written in Algol, and thoroughly tested with the Gier computer of the Warsaw University. This programme will be used in future in the stellar model computations. A slightly different version of it, written by Ziółkowski, was already utilized by Paczyński and Ziółkowski (1968a, b), and Ziółkowski (1968a, b). The second chapter of this paper is entirely devoted to the description of the computational

© Copernicus Foundation for Polish Astronomy • Provided by the NASA Astrophysics Data System

1969AcA....19....1P

technique used. Some results obtained with this programme for the red supergiant envelopes are given in the third chapter.

The programme described is available on request from the Institute of Astronomy, Polish Academy of Sciences, Warszawa, Al. Ujazdowskie 4, Poland on a paper tape punched on a Friden flexowriter.

2. Computational Technique

a) The radiative temperature gradient.

The atmosphere of a supergiant may have a thickness which is not very much smaller than the stellar radius. That means one cannot neglect the sphericity of such atmosphere even in a first approximation. Kosirev (1934) and Chandrasekhar (1934) studied the radiative transfer in the extended stellar atmospheres. They gave the following formula for an approximate dependence of the temperature on the optical depth τ

$$T^4 = \frac{L}{8\pi\sigma}\left[\frac{1}{R^2} + \frac{3}{2}\int_0^\tau \frac{d\tau}{r^2}\right] =$$

$$= \frac{L}{8\pi\sigma R^2}\left[1 + \frac{3}{2}\int_0^\tau \left(\frac{R}{r}\right)^2 d\tau\right], \tag{1}$$

where $d\tau = -\varkappa\varrho\, dr$, $\varkappa$ is the coefficient of opacity, ϱ is the density, r is the radius, L is the luminosity, and R is the radius at which $\tau = 0$. For the plane parallel atmosphere we have $r \approx R$ and Eq. (1) reduces to

$$T^4 = \frac{L}{8\pi\sigma R^2}\left(1 + \frac{3}{2}\tau\right). \tag{2}$$

This corresponds to the Eddington approximation. Formula (1) was used by Henyey, Vardya, and Bodenheimer (1965) in their computations of stellar envelopes. The surface temperature (at $\tau = 0$) is given as

$$T_0^4 = \frac{L}{8\pi\sigma R^2}\,. \tag{3}$$

Let us differentiate Eq. (1). We get

$$4\,T^3\frac{dT}{dr} = -\frac{3\,L\,\varkappa\varrho}{16\pi\sigma r^2}\,. \tag{4}$$

This is the well known formula for the temperature gradient in the diffusion approximation for the equation of radiative transfer. It is

© Copernicus Foundation for Polish Astronomy • Provided by the NASA Astrophysics Data System

1969AcA....19....1P

commonly used in the studies of stellar interiors, but is obviously inadequate for finding the structure of extended atmospheres. This is clearly demonstrated with the following example.

Let us consider an atmosphere with a boundary $\tau = 0$ at $r = R$. Let us have $\tau \ll 1$ at $R' \ll R$. According to Eq. (1) and Eq. (3) we should have almost the same temperature $T_0 = \left(\frac{L}{8\pi\sigma R^2}\right)^{1/4}$ at the two points, R' and R. Let us suppose now, that there is no opacity between R' and R. Then it is natural to adopt a boundary $\tau = 0$ at $r = R'$. In this case we should have at R' the temperature $T_0' = \left(\frac{L}{8\pi\sigma R'^2}\right)^{1/4}$ according to Eqs. (1) and (3). We have of course $T_0 \ll T_0'$. We see that a minor change of the opacity in the outermost atmosphere, or in fact the arbitrary choice of the boundary $\tau = 0$, results in a large uncertainty within the extended atmosphere. That is so because Eqs. (1) and (4) do not take the dilution of radiation into account.

Let us consider matter far from the star. If the coefficient of opacity of that matter were independent on the wavelength of radiation, we would there have the temperature given by

$$T = \left(\frac{L}{16\pi\sigma r^2}\right)^{1/4}, \tag{5}$$

where r is the distance from the star, and L is the luminosity. With no appreciable optical thickness of the matter considered there should be a temperature gradient due to the dilution of stellar radiation according to Eq. (5). Something similar should be present in the extended stellar atmosphere. Let us differentiate Eq. (5). Then we get

$$\frac{dT}{dr} = -0{\cdot}5\, T_0\, R_0^{1/2}\, r^{-3/2}, \tag{6}$$

where T_0 is the temperature at R_0 according to Eq. (5).

In our computations we adopted the following crude formula to compute the radiative temperature gradient in the atmosphere

$$\frac{dT}{dr} = -\frac{3\varkappa\varrho L}{64\pi\sigma r^2 T^3} - f \times 0{\cdot}5\, T_0\, R_0^{1/2} r^{-3/2}, \tag{7}$$

where

$$f = \begin{cases} 1 - \frac{3}{2}\tau & \text{for } \tau < \frac{2}{3}, \\ 0 & \text{for } \tau \geqslant \frac{2}{3}, \end{cases} \tag{8}$$

© Copernicus Foundation for Polish Astronomy • Provided by the NASA Astrophysics Data System

1969AcA....19....1P

and

$$\tau = \int_{r}^{R_0} \varkappa \varrho \, dr \,. \tag{9}$$

At the upper boundary of the atmosphere we adopted

$$T_0^4 = \frac{L}{8\pi\sigma R_0^2} \quad \text{and} \quad \tau = 0 \quad \text{at} \quad r = R_0 \tag{10}$$

The dilution of radiation was roughly accounted for with a second term on the right hand side of Eq. (7).

The temperature T_0 was computed by us similarly as in the case of a very thin atmosphere according to the Eddington approximation. This is not very consistent with our attempt to account for the temperature gradient due to the dilution effect. However, the conditions in the upper atmosphere are approximated by us so roughly, that we do not think that T_0 computed with Eq. (5) would be much better. The principal aim of our approximation was to get a formula for the temperature distribution in the atmosphere that would be independent of the choice of the position of the upper boundary, R_0.

The choice of the density ϱ_0 at the point R_0 is arbitrary as long as the density is sufficiently small. Of course, by taking two different densities at the same R_0 we shall get two different model atmospheres and envelopes. It is possible to get a model of the same atmosphere with many different pairs of ϱ_0, R_0, as long as the point ϱ_0, R_0, is at sufficiently small optical depth. This may be understood in the following manner. Let us take some R_0 and a very small ϱ_0 as the upper boundary, and let us integrate the equations describing the structure of the atmosphere. As a result we shall get the run of $\varrho(r)$ in our model. Let us take now a point at $R_0' < R_0$ as a boundary, let us adopt $\varrho_0' = \varrho(r)|_{r=R_0'}$ as the density corresponding to this boundary, and let us integrate the corresponding equations. The new model should be identical with the first one for $r < R_0'$, as long as $\tau(R_0') \ll 1$. With our choice of the dependence $T(\tau)$ this requirement was satisfied with a reasonable accuracy. It is easy to see that the approximation for $T(\tau)$ given by Kosirev and Chandrasekhar is very bad from this point of view.

b) The pressure gradient.

Let us write down the equations for the gradients of gas and radiation pressures

© Copernicus Foundation for Polish Astronomy • Provided by the NASA Astrophysics Data System

1969AcA....19....1P

$$\frac{dP_g}{dr} = -\frac{G\mathfrak{M}_r}{r^2}\varrho + \frac{\varkappa L}{4\pi c r^2}\varrho\,,$$
$$\frac{dPr}{dr} = \frac{4}{3} a T^3 \frac{dT}{dr}\,. \tag{11}$$

If Eddington approximation were used for the temperature gradient, we would have

$$\frac{dP}{dr} \equiv \frac{d(P_g + P_r)}{dr} = -\frac{G\mathfrak{M}_r}{r^2}\varrho\,. \tag{12}$$

With our formula for the radiative temperature gradient (Eq. 7), we have

$$\frac{dP}{dr} = -\frac{G\mathfrak{M}_r}{r^2}\rho\left[1 + f\frac{2 a T^3 r^{1/2}}{3 G \mathfrak{M}_r \varrho}\left(\frac{L}{8\pi\sigma}\right)^{1/4}\right] \tag{13}$$

To test the convective stability of the model atmosphere it is necessary to have an expression for the radiative gradient of the logarithm of the temperature with respect to the logarithm of pressure. In our case we have

$$\nabla_{rad} \equiv \left(\frac{d\ln T}{d\ln P}\right)_{rad} = \frac{\varkappa L}{16\pi G c (1-\beta)\mathfrak{M}_r}\frac{\left(1 + f s\frac{4\pi G c \mathfrak{M}_r}{\varkappa L}\right)}{(1 + f s)}, \tag{14}$$

$$\beta = \frac{P_g}{P} \quad \text{and} \quad s = \frac{2 a T^3 r^{1/2}}{3 G \mathfrak{M}_r \varrho}\left(\frac{L}{8\pi\sigma}\right)^{1/4}. \tag{15}$$

c) The convective gradient.

We can easily compute the radiative gradient in the atmosphere and in the stellar envelope by means of Eq. (14). It is also easy to compute the adiabatic gradient $\nabla_{ad} \equiv (d\ln T/d\ln P)_{ad}$. Here we shall present in some details the computational scheme for finding the convective gradient within the framework of the mixing length theory. This is necessary whenever $\nabla_{ad} < \nabla_{rad}$. Let us write down the full set of equations used for this purpose (*cf.* Kippenhahn 1963, Henyey, Vardya and Bodenheimer 1965, Baker and Temesváry 1966, p. 60).

$$F_r \equiv \frac{L_r}{4\pi r^2} = F_{rad} + F_{conv} = \frac{16\sigma T^4}{3\varkappa\varrho H_p}\nabla_{rad}\,, \tag{16}$$

$$F_{rad} = \frac{16\sigma T^4}{3\varkappa\varrho H_p}\nabla_{conv}\,, \tag{17}$$

© Copernicus Foundation for Polish Astronomy • Provided by the NASA Astrophysics Data System

1969AcA....19....1P

$$F_{\rm conv} = \frac{1}{2} c_p \varrho T v_t \frac{l_t}{H_p} (\nabla_{\rm conv} - \nabla') , \tag{18}$$

$$v_t^2 = \frac{g l_t^2}{8 H_p} Q (\nabla_{\rm conv} - \nabla') , \tag{19}$$

$$\frac{\nabla_{\rm conv} - \nabla'}{\nabla' - \nabla_{ad}} = \gamma_0 v_t , \tag{20}$$

where

$$Q = -\left(\frac{\partial \ln \varrho}{\partial \ln T}\right)_P , \quad \gamma_0 = \frac{c_p \varrho}{8 \sigma T^3} \frac{1 + \frac{1}{3}\omega^2}{\omega} ,$$
$$\omega = \varkappa \varrho l_t , \quad g = \frac{G \mathfrak{M}_r}{r^2} , \tag{21}$$

and $\nabla_{\rm conv}$ is the actual, convective gradient $(d \ln T / d \ln P)_{\rm conv}$. All other symbols have their usual meaning. In the formulae presented above the optically thin and thick turbulent elements are treated following Henyey *et al.* (1965).

Let us introduce new parameters

$$C = \frac{g l_t^2 Q}{8 H_p} , \quad V = \frac{1}{\gamma_0 C^{1/2} (\nabla_{\rm rad} - \nabla_{\rm ad})^{1/2}} , \quad A = \frac{9}{8} \frac{\omega^2}{3 + \omega^2} , \tag{22}$$

and a variable

$$y = v_t V \gamma_0 . \tag{23}$$

It is easy to show that Eqs. (16—20) may be reduced to a single cubic equation for y

$$2 A y^3 + V y^2 + V^2 y - V = 0 . \tag{24}$$

One may notice that our y corresponds to Kippenhahn's (1963) $(\sqrt{\nabla - \nabla_{\rm ad} + U^2} - U)/\sqrt{\nabla_{\rm rad} - \nabla_{\rm ad}}$, our V to Kippenhahn's $2U/\sqrt{\nabla_{\rm rad} - \nabla_{\rm ad}}$, and our A to Kippenhahn's 9/8, as Kippenhahn considered only the case of optically thick turbulent elements.

It can be shown that there is always one real and positive root of Eq. (24), and that this root is always smaller than 1. We may write in general

$$y = y(A, V) . \tag{25}$$

This root may be found by means of iterations

$$y_0 = 1 ,$$
$$y_{n+1} = y_n - (B y_n^3 + y_n^2 + V y_n - 1)/(3 B y_n^2 + 2 y_n + V) , \tag{26}$$

© Copernicus Foundation for Polish Astronomy • Provided by the NASA Astrophysics Data System

1969AcA....19....1P

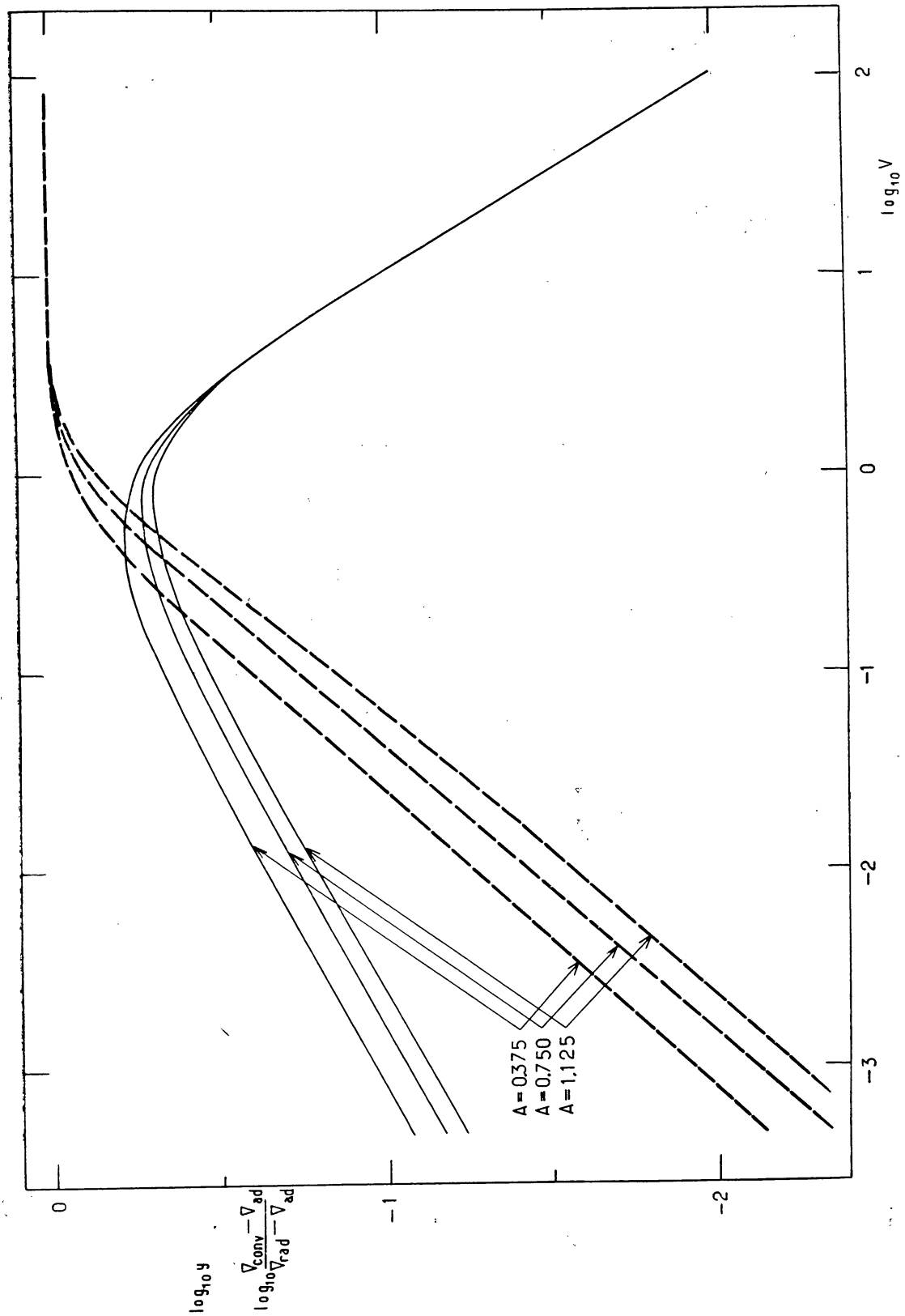

Fig. 1. The variation of $\log_{10} y$ (solid lines) and of $\log_{10}[(\nabla_{\mathrm{conv}} - \nabla_{\mathrm{ad}})/(\nabla_{\mathrm{rad}} - \nabla_{\mathrm{ad}})]$ (broken lines) with $\log_{10} V$ for three values of A is shown. See text for explanation of different symbols.

© Copernicus Foundation for Polish Astronomy • Provided by the NASA Astrophysics Data System

1969AcA....19....1P

where $B = 2A/V$. The march of y with A and V is shown in Fig. 1. We have $y \approx 1/V$ for $V \gg 1$, and $y \approx (V/2A)^{1/3}$ for $V \ll 1$.

Once y was found we readily get the mean turbulent velocity v_t, and the convective gradient ∇_{conv}

$$v_t = \frac{y}{V\gamma_0}, \quad \text{and} \quad \nabla_{conv} = \nabla_{ad} + (\nabla_{rad} - \nabla_{ad})\, y\,(y+V). \tag{27}$$

d) The density gradient.

We found it very convenient from the computational point of view to calculate the density gradient explicitely while integrating the equations of the atmosphere and envelope structure. We always may write

$$dP = \left(\frac{\partial P}{\partial \varrho}\right)_T d\varrho + \left(\frac{\partial P}{\partial T}\right)_\varrho dT, \tag{28}$$

and

$$\frac{d\varrho}{dr} = \left[\frac{dP}{dr} - \left(\frac{\partial P}{\partial T}\right)_\varrho \frac{dT}{dr}\right] \Big/ \left(\frac{\partial P}{\partial \varrho}\right)_T, \tag{29}$$

or

$$\nabla_\varrho \equiv \frac{d\ln\varrho}{d\ln P} = \left[P - \left(\frac{\partial P}{\partial T}\right)_\varrho T\nabla\right] \Big/ \left(\frac{\partial P}{\partial \varrho}\right)_T \Big/ \varrho, \tag{30}$$

where

$$\nabla = \begin{cases} \nabla_{rad} & \text{if } \nabla_{rad} \leqslant \nabla_{ad}, \\ \nabla_{conv} & \text{if } \nabla_{rad} > \nabla_{ad}. \end{cases} \tag{31}$$

e) Equations of structure of the atmosphere and envelope.

We adopted $\mathfrak{M} - \mathfrak{M}_r$ as the independent variable, $\mathfrak{M}$ being the total mass of a star. The radius r, temperature T, density ϱ, and optical thickness τ were taken as the dependent variables. The following equations were integrated

$$\begin{aligned} \frac{dT}{d(\mathfrak{M}-\mathfrak{M}_r)} &= \nabla \frac{T}{P}\frac{dP}{d(\mathfrak{M}-\mathfrak{M}_r)}, \\ \frac{d\varrho}{d(\mathfrak{M}-\mathfrak{M}_r)} &= \nabla_\varrho \frac{\varrho}{P}\frac{dP}{d(\mathfrak{M}-\mathfrak{M}_r)}, \\ \frac{dr}{d(\mathfrak{M}-\mathfrak{M}_r)} &= -\frac{1}{4\pi r^2 \varrho}, \\ \frac{d\tau}{d(\mathfrak{M}-\mathfrak{M}_r)} &= \frac{\varkappa}{4\pi r^2}, \end{aligned} \tag{32}$$

© Copernicus Foundation for Polish Astronomy • Provided by the NASA Astrophysics Data System

1969AcA....19....1P

where

$$\frac{dP}{d(\mathfrak{M}-\mathfrak{M}_r)} = \frac{G\mathfrak{M}_r}{4\pi r^4}(1+f\cdot s),$$
$$f = \begin{cases} 1-{}^3/_2\,\tau & \text{for } \tau < {}^2/_3 \\ 0 & \text{for } \tau \geqslant {}^2/_3 \end{cases} \qquad (33)$$
$$s = \frac{2aT^3 r^{1/2}}{3G\mathfrak{M}_r \varrho}\left(\frac{L}{8\pi\sigma}\right)^{1/4},$$

and ∇_ϱ and ∇ are given with Eqs. (30) and (31). The integrations were started with

$$\mathfrak{M}-\mathfrak{M}_r = 0\,.$$
$$T = \left(\frac{L}{8\pi\sigma R_0^2}\right)^{1/4},$$
$$\varrho = 10^{-12}\ \mathrm{g/cm^3}, \qquad (34)$$
$$r = R_0\,,$$
$$\tau = 0\,,$$

The integrations were stopped when one of the following conditions was fulfilled

$$T > T_{\max}\,,$$
$$\mathfrak{M}_r < 0{\cdot}1\,\mathfrak{M}\,, \qquad (35)$$
$$\varrho > 10 \quad \text{or} \quad \varrho < 10^{-12}\,.$$

$T_{\max}$ was usually taken as $5\times 10^5\,^\circ$K. In this way it was possible to integrate Eqs. (32) very deep into the interior of a supergiant star. In most cases the point at $r < 0{\cdot}05\,R_0$ was reached, and practically all the mass of an envelope was covered. The step of integration was taken so as to have an upper limit on the changes in one step of the variables $\mathfrak{M}_r$, T, ϱ, r, and also τ for $\tau < {}^2/_3$. We found that the numerical errors of our computations were comparable in magnitude to the results of a 10% change in the mixing length, for a maximum change in one step

$$\Delta\mathfrak{M}_r/\mathfrak{M}_r = 0{\cdot}5\,,$$
$$\Delta T/T = 0{\cdot}2\,,$$
$$\Delta\varrho/\varrho = 0{\cdot}5\,, \qquad (36)$$
$$\Delta r/r = 0{\cdot}2\,,$$
$$\Delta\tau/\tau = 0{\cdot}2\,, \quad \text{for } \tau < {}^2/_3\,.$$

In this way about 50 steps were needed to cover a typical atmosphere and envelope up to $T = 5\times 10^5\,^\circ$K.

© Copernicus Foundation for Polish Astronomy • Provided by the NASA Astrophysics Data System

1969AcA....19....1P

A very simple algorithm was used for the numerical integrations. We shall explain using as an example the equation

$$\frac{dy}{dx} = f(x, y) . \tag{37}$$

Given the values of x and y at the point n (i. e. given x_n and y_n) and the step size Δx, we calculate x_{n+1} and y_{n+1} at the point $n+1$ in the following manner

$$\begin{aligned} x' &= x_n + \frac{1}{2}\Delta x , \\ y' &= y_n + \frac{1}{2} f(x_n, y_n)\,\Delta x , \\ x_{n+1} &= x_n + \Delta x , \\ y_{n+1} &= y_n + f(x', y')\,\Delta x . \end{aligned} \tag{38}$$

f) Thermodynamic functions.

We had the density ϱ, and the temperature T at every point in the atmosphere or envelope given as a direct result of numerical integrations of Eqs. (32). Given ϱ and T we calculate the pressure P and the internal energy per gram U. Subsequently the derivatives

$$\left(\frac{\partial P}{\partial \varrho}\right)_T , \quad \left(\frac{\partial P}{\partial T}\right)_\varrho , \quad \left(\frac{\partial U}{\partial \varrho}\right)_T , \quad \left(\frac{\partial U}{\partial T}\right)_\varrho \tag{39}$$

were computed numerically, varying ϱ and T by 0·1% of their values. All other thermodynamic functions may be readily obtained by the formulae

$$\begin{aligned} Q &\equiv -\left(\frac{\partial \ln \varrho}{\partial \ln T}\right)_P = \frac{T}{\varrho}\left(\frac{\partial P}{\partial T}\right)_\varrho \Big/ \left(\frac{\partial P}{\partial \varrho}\right)_T \\ c_V &= \left(\frac{\partial U}{\partial T}\right)_\varrho \\ c_P &= c_V + \frac{Q}{\varrho}\left(\frac{\partial P}{\partial T}\right)_\varrho \\ \nabla_{ad} &= \frac{PQ}{\varrho\, T\, c_P} , \\ V_t &= \left(\frac{\partial P}{\partial \varrho}\right)_T^{1/2} \qquad \text{(isothermal sound velocity)} , \\ V_{ad} &= V_t \left(\frac{c_P}{c_V}\right)^{1/2} \qquad \text{(adiabatic sound velocity)} . \end{aligned} \tag{40}$$

© Copernicus Foundation for Polish Astronomy • Provided by the NASA Astrophysics Data System

1969AcA....19....1P

In this way it is sufficient to have an algorithm for finding $P(\varrho, T)$ and $U(\varrho, T)$ and all the remaining computations of the thermodynamic functions are very simple. In all our calculations U, c_P, and c_V were computed per one gram of the gas and radiation mixture.

In calculating P and U we took into account the gas and radiation pressures, the ionization of H I, He I, and He II, and the dissociation of the H_2 molecule. We did not calculate accurately the concentrations of species that were not abundant in the relevant range of densities and temperatures. We have used the same basic equations and constants as Vardya (1960, Eqs. 6·16 — 6·19). The computations proceeded in the following way

1. Ionization of hydrogen was calculated neglecting the existence of the H_2 molecule and the ionization of helium. The first approximation for the electron density (N_e) was obtained assuming that all the electrons are supplied by the ionized hydrogen.

2. First ionization of helium was computed neglecting the second ionization of this element. Free electrons were assumed to come from the hydrogen and the singly ionized helium.

3. Second helium ionization was calculated with N_e coming from all degrees of ionization of hydrogen and helium. The final (third) approximation to N_e was obtained.

4. Concentration of the H_2 molecule was found taking the amount of neutral hydrogen as obtained in the first step of this procedure.

In principle this procedure may be repeated many times to get any desired accuracy. We found that a reasonable accuracy may be obtained in a single cycle of this procedure for all the densities and temperatures of interest.

Let us denote the number of different particles in one cubic centimeter as *NH2*, *NHI*, *NHII*, *NHEI*, *NHEII*, *NHEIII*, *NE*, and *NT* for the hydrogen molecules, neutral and ionized hydrogen and helium, free electrons, and a total number of particles respectively. We neglect the concentration of heavier elements at this point. Then we have in c. g. s. units

$$
\begin{aligned}
P_g &= 1{\cdot}3805 \times 10^{-16} \times T \times NT\,, \\
P_r &= 2{\cdot}523 \times 10^{-15} \times T^4\,, \\
P &= P_g + P_r\,, \\
U &= (1{\cdot}5 \times P_g + 3 \times P_r + 1{\cdot}3805 \times 10^{-16} \times NH2 \times UH2 + \\
&\quad + 3{\cdot}585 \times 10^{-12} \times NHI + 25{\cdot}36 \times 10^{-12} \times NHII + \\
&\quad + 39{\cdot}37 \times 10^{-12} \times NHEII + 126.52 \times 10^{-12} \times NHEIII)/\varrho\,,
\end{aligned}
\tag{41}
$$

© Copernicus Foundation for Polish Astronomy • Provided by the NASA Astrophysics Data System

1969AcA....19....1P

where

$$UH2 = \begin{cases} 2{\cdot}1 \times T + 2{\cdot}5 \times 10^{-4} \times T^2 & \text{for} \quad T < 3000^\circ\text{K}, \\ -1890 + 3{\cdot}36 \times T + 4 \times 10^{-5} \times T^2 & \text{for} \quad T > 3000^\circ\text{K}, \end{cases} \tag{42}$$

is the internal energy of one H_2 molecule. The formula (42) was fitted to Table 1 of Vardya (1960). For the temperature $T > 12\,000^\circ$K the abundance of H_2 was artificially cut down following a recomendation by Vardya (1960).

For high temperature and low density complete ionization was assumed, and a mixture of fully ionized perfect gas and radiation was considered. This was done when the condition

$$-\frac{630\,908}{T} + 1{\cdot}5 \ln T - \ln \varrho > 26{\cdot}5 \tag{43}$$

was fulfilled, i. e. when the percentage of the twice ionized helium was 99·9% or more. In this case all the basic thermodynamic functions were computed as follows

$$P_1 = 0{\cdot}825 \times 10^8 (2X + 0{\cdot}75\,Y),$$

$$P_2 = 2{\cdot}523 \times 10^{-15}\, T^3/\varrho,$$

$$P = (P_1 + P_2)\,\varrho\, T,$$

$$U = (1{\cdot}5\,P_1 + 3\,P_2)\,T + 1{\cdot}516 \times 10^{13}\,X + 1{\cdot}890 \times 10^{13}\,Y,$$

$$\left(\frac{\partial P}{\partial \varrho}\right)_T = P_1 \times T, \tag{44}$$

$$\left(\frac{\partial P}{\partial T}\right)_\varrho = (P_1 + 4\,P_2)\,\varrho,$$

$$\left(\frac{\partial U}{\partial \varrho}\right)_T = -3\,P_2 \times T/\varrho,$$

$$\left(\frac{\partial U}{\partial T}\right)_\varrho = 1{\cdot}5\,P_1 + 12\,P_2,$$

where X and Y denote the hydrogen and helium content by mass, respectively.

Adopting the density and the temperature as the basic dependent variables we were able to derive all the thermodynamic functions needed without making iterations at any part of our computations. We got as a result a fast and simple computer programme.

© Copernicus Foundation for Polish Astronomy • Provided by the NASA Astrophysics Data System

1969AcA....19....1P

g) Coefficient of opacity.

We have adopted the opacities published by Baker and Temesváry (1966, Table 94) for $X = 0{\cdot}70$, $Y = 0{\cdot}27$, $Z = 0{\cdot}03$. In addition we took the opacity due to the H_2O molecule into account. The Rosseland mean opacity of H_2O may be computed from the tables published by Auman (1967). We found that for the temperature range $1680 - 3360°K$ this mean does not vary by more than 30% and is approximately equal to $0{\cdot}3$ cm²/g of H_2O for the turbulence of 4 km/sec. Thus we have

$$\varkappa_{H_2O} \approx 0{\cdot}3\, X_{H_2O} \tag{45}$$

in c. g. s. units, where X_{H_2O} is the H_2O content by mass. The concentration of the H_2O molecule was tabulated by Tsuji (1964) for a variety of chemical compositions of stellar atmosphere. We adopted his case I, that is the mass ratio carbon : nitrogen : oxygen $= 5 \times 10^{-4} : 10^{-4} : 10^{-3}$, which is very close to that used by Baker and Temesváry (1966) in their opacity table. It is possible to approximate the tables of Tsuji with an accuracy better than 25% in the important range of densities and temperatures with a formula

$$\log_{10} X_{H_2O} = \log_{10} X_{CNO} - 0{\cdot}41 + f(x)\,, \tag{46}$$

where X_{CNO} is a total abundance of the carbon, nitrogen and oxygen by mass, and

$$f(x) = 5\,[x - \mathrm{abs}\,(x)] - 0{\cdot}64 \exp\,[-7{\cdot}8\ \mathrm{abs}\,(x)]\,,$$

$$x = \frac{5040}{T} + 0{\cdot}2 \log_{10}\left(\frac{k}{H}\,\varrho\, T\, X\right) - 2{\cdot}493\,, \tag{47}$$

and all other symbols have their usual meaning. The opacity due to the H_2O molecule is therefore given by the formula

$$\log \varkappa_{H_2O} = \log_{10} X_{CNO} - 0{\cdot}9 + f(x)\,. \tag{48}$$

The opacity so obtained was added to that tabulated by Baker and Temesváry. We have finally used our Table 1 in the computations. The logarithm of the opacity coefficient was interpolated linearly in the $\log \varrho$ and $\log T$. The variation of the coefficient of opacity with the density and temperature is shown in Fig. 1 of Paczyński (1968).

3. Results of computations

Almost two hundred model envelopes were calculated for red supergiants with masses in the range of $0{\cdot}5 - 16\ \mathfrak{M}_\odot$. Here we present the results for $1\ \mathfrak{M}_\odot$. The envelopes of stars with different masses had

© Copernicus Foundation for Polish Astronomy • Provided by the NASA Astrophysics Data System

1969AcA....19....1P

Table 1.

Logarithm of the Coefficient of Opacity
for $X = 0{\cdot}70$, $Y = 0{\cdot}27$, $Z = 0{\cdot}03$.

LOG RHO / LOG T	-12	-11	-10	-9	-8	-7	-6	-5	-4	-3	-2	-1	0	1
3.30	-2.63	-2.63	-2.63	-2.63	-2.63	-2.61	-2.58	-2.45	0.00	0.00	0.00	0.00	0.00	0.00
3.35	-2.63	-2.63	-2.63	-2.63	-2.62	-2.59	-2.46	-2.16	0.00	0.00	0.00	0.00	0.00	0.00
3.40	-2.74	-2.65	-2.64	-2.63	-2.61	-2.51	-2.25	-1.82	0.00	0.00	0.00	0.00	0.00	0.00
3.45	-3.17	-2.74	-2.65	-2.62	-2.56	-2.32	-1.96	-1.41	0.00	0.00	0.00	0.00	0.00	0.00
3.50	-4.30	-3.11	-2.72	-2.62	-2.50	-2.10	-1.58	-0.96	-0.38	0.00	0.00	0.00	0.00	0.00
3.55	-4.46	-3.96	-2.96	-2.64	-2.41	-1.86	-1.18	-0.54	0.02	0.00	0.00	0.00	0.00	0.00
3.60	-4.20	-4.24	-3.48	-2.68	-2.25	-1.68	-0.96	-0.21	0.41	0.00	0.00	0.00	0.00	0.00
3.65	-3.50	-3.78	-3.54	-2.79	-2.08	-1.43	-0.77	-0.03	0.67	0.00	0.00	0.00	0.00	0.00
3.70	-2.72	-3.09	-3.09	-2.58	-1.92	-1.22	-0.53	0.13	0.82	1.39	0.00	0.00	0.00	0.00
3.75	-1.90	-2.27	-2.46	-2.09	-1.59	-0.97	-0.31	0.34	0.96	1.53	0.00	0.00	0.00	0.00
3.80	-1.23	-1.51	-1.70	-1.40	-0.99	-0.51	0.05	0.60	1.18	1.71	0.00	0.00	0.00	0.00
3.85	-0.68	-0.81	-0.86	-0.69	-0.37	0.00	0.42	0.91	1.43	1.92	0.00	0.00	0.00	0.00
3.90	-0.57	-0.49	-0.30	-0.02	0.25	0.53	0.88	1.31	1.76	2.22	0.00	0.00	0.00	0.00
3.95	-0.48	-0.17	0.29	0.64	0.85	1.06	1.34	1.69	2.07	2.51	0.00	0.00	0.00	0.00
4.00	-0.47	-0.13	0.50	1.08	1.38	1.56	1.77	2.05	2.39	2.79	0.00	0.00	0.00	0.00
4.05	-0.48	-0.22	0.40	1.14	1.66	1.98	2.16	2.38	2.68	3.03	0.00	0.00	0.00	0.00
4.10	-0.48	-0.30	0.22	1.04	1.80	2.38	2.54	2.72	2.96	3.27	0.00	0.00	0.00	0.00
4.15	-0.49	-0.36	0.08	0.85	1.72	2.44	2.78	3.00	3.22	3.47	0.00	0.00	0.00	0.00
4.20	-0.49	-0.40	-0.04	0.64	1.53	2.38	2.96	3.24	3.44	3.65	0.00	0.00	0.00	0.00
4.25	-0.49	-0.42	-0.14	0.47	1.35	2.22	2.93	3.36	3.62	3.82	0.00	0.00	0.00	0.00
4.30	-0.49	-0.43	-0.23	0.30	1.16	2.05	2.88	3.48	3.80	3.99	0.00	0.00	0.00	0.00
4.35	-0.48	-0.43	-0.25	0.22	1.02	1.93	2.80	3.48	3.90	4.16	0.00	0.00	0.00	0.00
4.40	-0.48	-0.42	-0.26	0.15	0.90	1.81	2.72	3.48	4.01	4.33	0.00	0.00	0.00	0.00
4.45	-0.47	-0.42	-0.27	0.08	0.78	1.70	2.64	3.47	4.11	4.50	0.00	0.00	0.00	0.00
4.50	-0.47	-0.42	-0.30	0.03	0.72	1.62	2.57	3.45	4.16	4.63	0.00	0.00	0.00	0.00
4.55	-0.47	-0.44	-0.33	0.00	0.67	1.56	2.51	3.42	4.20	4.75	0.00	0.00	0.00	0.00
4.60	-0.47	-0.45	-0.36	-0.04	0.63	1.50	2.45	3.39	4.24	4.87	0.00	0.00	0.00	0.00
4.65	-0.47	-0.46	-0.39	-0.08	0.57	1.42	2.37	3.34	4.25	4.95	4.96	0.00	0.00	0.00
4.70	-0.47	-0.46	-0.42	-0.17	0.40	1.26	2.23	3.21	4.12	4.84	4.92	0.00	0.00	0.00
4.75	-0.47	-0.46	-0.43	-0.26	0.24	1.10	2.09	3.08	4.00	4.74	4.88	0.00	0.00	0.00
4.80	-0.47	-0.47	-0.44	-0.31	0.14	0.94	1.90	2.89	3.82	4.58	4.79	0.00	0.00	0.00
4.85	-0.47	-0.47	-0.45	-0.34	0.06	0.78	1.70	2.68	3.62	4.40	4.70	0.00	0.00	0.00
4.90	-0.47	-0.47	-0.45	-0.36	-0.03	0.62	1.50	2.48	3.42	4.23	4.60	0.00	0.00	0.00
4.95	-0.47	-0.47	-0.46	-0.39	-0.11	0.47	1.32	2.28	3.24	4.06	4.50	0.00	0.00	0.00
5.00	-0.47	-0.47	-0.46	-0.41	-0.19	0.32	1.14	2.09	3.04	3.90	4.40	0.00	0.00	0.00
5.20	-0.47	-0.47	-0.47	-0.46	-0.40	-0.10	0.59	1.50	2.46	3.28	3.88	3.92	0.00	0.00
5.40	-0.47	-0.47	-0.47	-0.47	-0.46	-0.38	-0.01	0.73	1.61	2.48	3.08	3.37	0.00	0.00
5.60	-0.47	-0.47	-0.47	-0.47	-0.47	-0.46	-0.37	0.01	0.77	1.66	2.36	2.78	3.11	0.00
5.80	-0.47	-0.47	-0.47	-0.47	-0.47	-0.47	-0.46	-0.33	0.12	0.95	1.76	2.30	2.72	0.00
6.00	-0.47	-0.47	-0.47	-0.47	-0.47	-0.47	-0.47	-0.43	-0.25	0.28	1.11	1.84	2.33	2.49
6.20	-0.47	-0.47	-0.47	-0.47	-0.47	-0.47	-0.47	-0.46	-0.39	-0.12	0.55	1.35	1.99	2.26
6.40	-0.47	-0.47	-0.47	-0.47	-0.47	-0.47	-0.47	-0.47	-0.44	-0.34	0.09	0.84	1.52	1.86
6.60	-0.47	-0.47	-0.47	-0.47	-0.47	-0.47	-0.47	-0.47	-0.47	-0.45	-0.29	0.21	0.84	1.26
6.80	-0.47	-0.47	-0.47	-0.47	-0.47	-0.47	-0.47	-0.47	-0.47	-0.47	-0.45	-0.29	0.14	0.60
7.00	-0.47	-0.47	-0.47	-0.47	-0.47	-0.47	-0.47	-0.47	-0.47	-0.47	-0.47	-0.44	-0.30	0.03
7.20	-0.47	-0.47	-0.47	-0.47	-0.47	-0.47	-0.47	-0.47	-0.47	-0.47	-0.48	-0.48	-0.44	-0.30
7.40	-0.47	-0.47	-0.47	-0.47	-0.47	-0.47	-0.47	-0.47	-0.47	-0.47	-0.49	-0.49	-0.48	-0.44

© Copernicus Foundation for Polish Astronomy • Provided by the NASA Astrophysics Data System

1969AcA....19....1P

the properties qualitatively similar to those found for $1\,\mathfrak{M}_\odot$. We adopted the composition $X = 0{\cdot}70$, $Y = 0{\cdot}27$, and $Z = 0{\cdot}03$, and the computer programme described in the previous chapter was used. All the computations were performed with the Gier computer of the Warsaw University. It took about 4—5 minutes to obtain a single envelope model.

A number of models with a luminosity $L = 6000\,L_\odot$ were computed with and without the opacity due to the H_2O molecules. For a given fraction of mass contained in the core, the models with H_2O had much

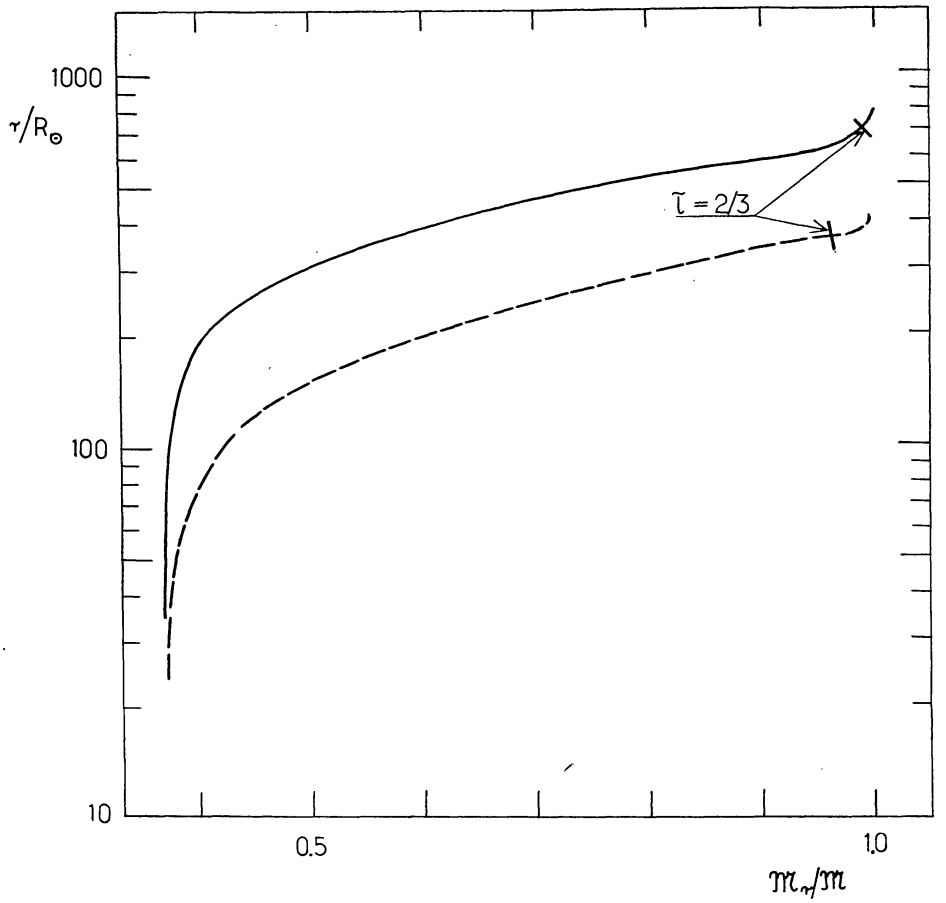

Fig. 2. The variation of the radius as a function of the mass fraction is shown for a star of $\mathfrak{M} = 1\,\mathfrak{M}_\odot$, $\mathfrak{M}_{core} = 0{\cdot}37\,\mathfrak{M}_\odot$, and $L = 6000\,L_\odot$. The solid line is for a model with the opacity due to H_2O included, and the broken line if for a model without H_2O. The arrows show the position of the photosphere.

more extended envelopes than the models without H_2O. Variation of the mass fraction of the core in the range of $0{\cdot}37 - 0{\cdot}95$ caused a variation of the envelope radius in the range of $360 - 240\,R_\odot$ for the models without H_2O, and in the range of $700 - 330\,R_\odot$ for the models

© Copernicus Foundation for Polish Astronomy • Provided by the NASA Astrophysics Data System

1969AcA....19....1P

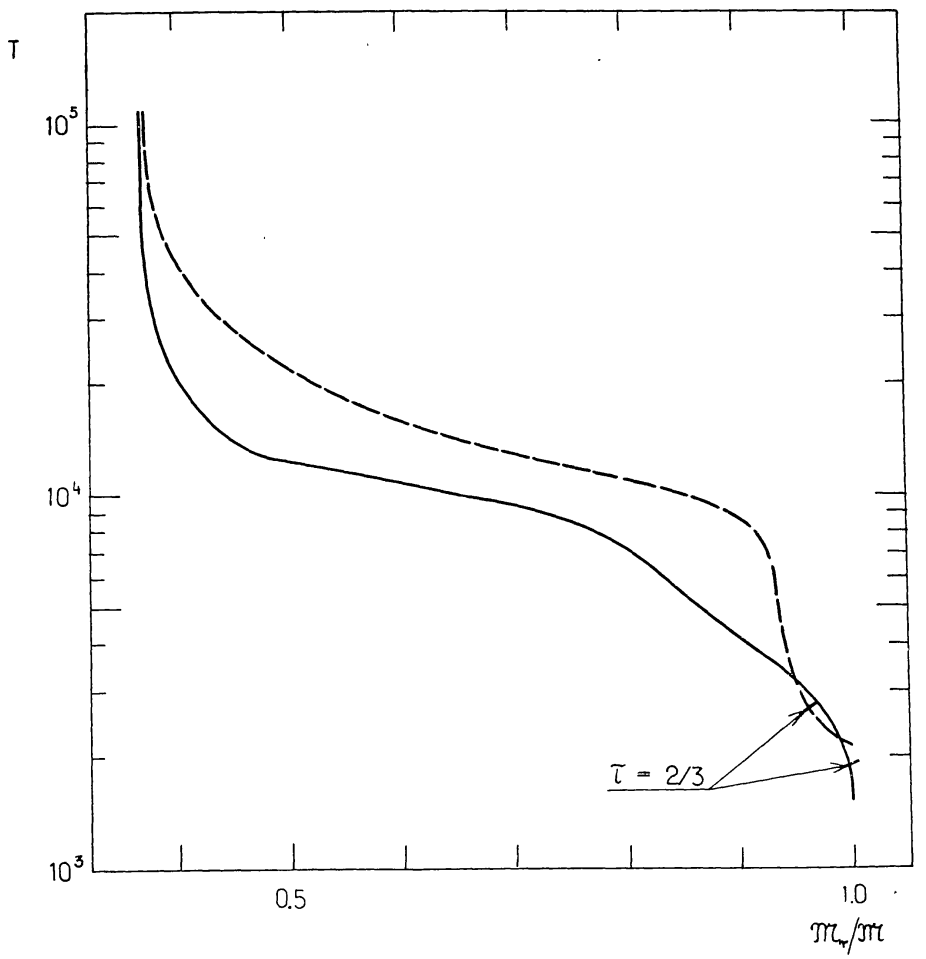

Fig. 3. The variation of the temperature as a function of mass fraction is shown for a star of $\mathfrak{M} = 1\,\mathfrak{M}_\odot$, $\mathfrak{M}_{core} = 0{\cdot}37\,\mathfrak{M}_\odot$, and $L = 6000\,L_\odot$. The solid line is for a model with the opacity due to H_2O included, and the broken line is for a model without H_2O. The arrows show the position of the photosphere.

with H_2O. The changes in the photospheric temperature were 2650°K — — 3450°K, and 1900°K — 2730°K, respectively. By the photosphere we understand here the layer at optical depth $\tau = 2/3$. We would like to point out that not only the photospheric temperatures of the models with H_2O are considerably lower, but also the relative change of the temperature is larger, when the mass of the core is varied. The former result is in agreement with that published by Auman and Bodenheimer (1967) and also by Kamijo (1968).

The differences between the envelopes with and without H_2O are shown in Figures 2 — 4 for the models with a core of $0{\cdot}37\,\mathfrak{M}_\odot$. The variations of the density and the temperature are much smoother in

© Copernicus Foundation for Polish Astronomy • Provided by the NASA Astrophysics Data System

1969AcA....19....1P

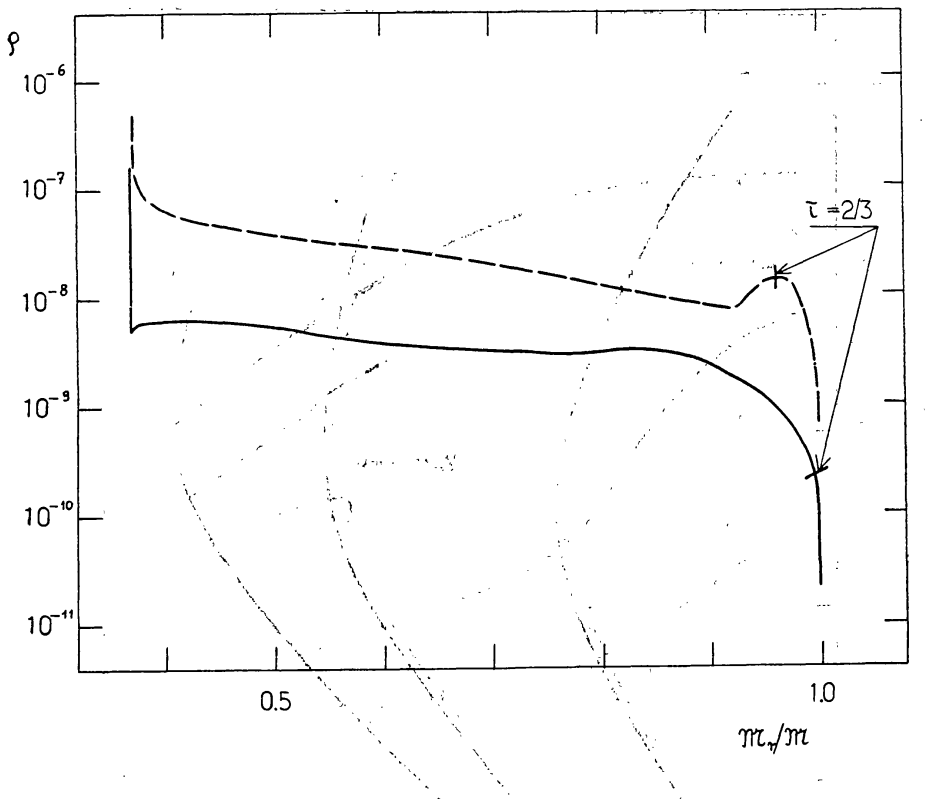

Fig. 4. The variation of the density as a function of mass fraction is shown for a star of $\mathfrak{M} = 1\,\mathfrak{M}_\odot$, $\mathfrak{M}_{core} = 0{\cdot}37\,\mathfrak{M}_\odot$, and $L = 6000\,L_\odot$. The solid line is for a model with the opacity due to H_2O included, and the broken line is for a model without H_2O. The arrows show the position of the photosphere.

the model with H_2O, because this envelope is more extended, has much smaller average density, and therefore has more smooth variation of the opacity coefficient (*cf.* Fig. 1 of Paczyński 1968). One may easily notice, that the fraction of mass contained in the atmosphere, that is above the optical depth 2/3, is about 5 — 8 times larger in the model without H_2O. That is because the opacity in this atmosphere is much smaller, and a large amount of mass is needed to have an optical thickness of 2/3.

The position of the envelopes with H_2O on the H — R diagram and various parameters for these envelopes and their atmospheres are displayed in Figures 5 — 7. We may see in Fig. 5 that the total energy of an envelope is positive, if the model has a luminosity larger than $M_{bol} = -3{\cdot}5$ or -4. The largest energies correspond to the kinetic energy of the envelope moving with a velocity slightly higher than 30 km/sec. We have shown previously (Paczyński and Ziółkowski 1968a, b) that the envelopes are dynamically unstable, if the luminosity

© Copernicus Foundation for Polish Astronomy • Provided by the NASA Astrophysics Data System

1969AcA....19....1P

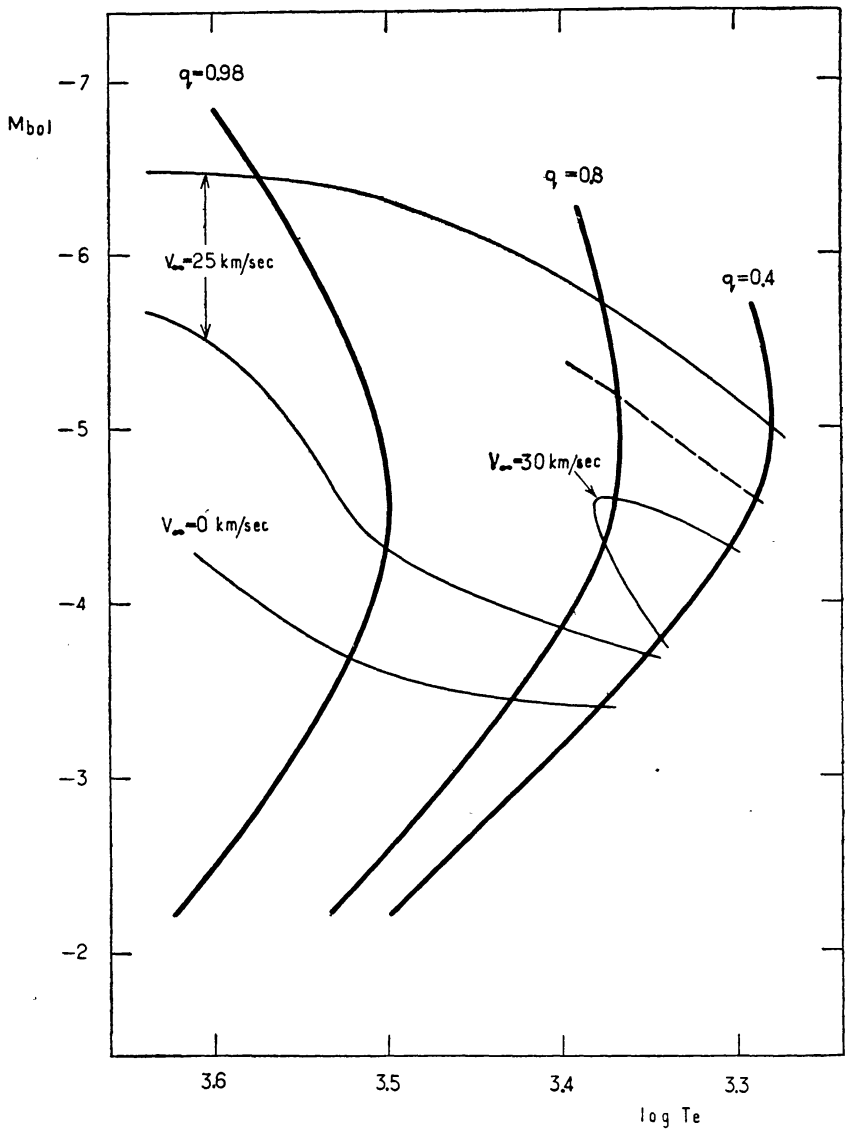

Fig. 5. The position of the model envelopes on the H—R diagram for a star of $1\,\mathfrak{M}_{\odot}$. Thick solid lines show the position of the models with a given fraction of mass q contained in the core. The borderline for dynamically unstable envelopes is shown after Paczyński and Ziółkowski (1968a). For the envelopes with the total energy being positive, the velocity giving the kinetic energy of the envelope equal to the total energy is marked (thin solid lines).

of the star is above certain limit. The borderline for dynamically unstable envelopes is shown in Fig. 5 with the broken line. The total energy of the typical envelope close to that borderline is sufficient to expel that envelope up to infinity at a speed of 28 km/sec.

© Copernicus Foundation for Polish Astronomy • Provided by the NASA Astrophysics Data System

1969AcA....19....1P

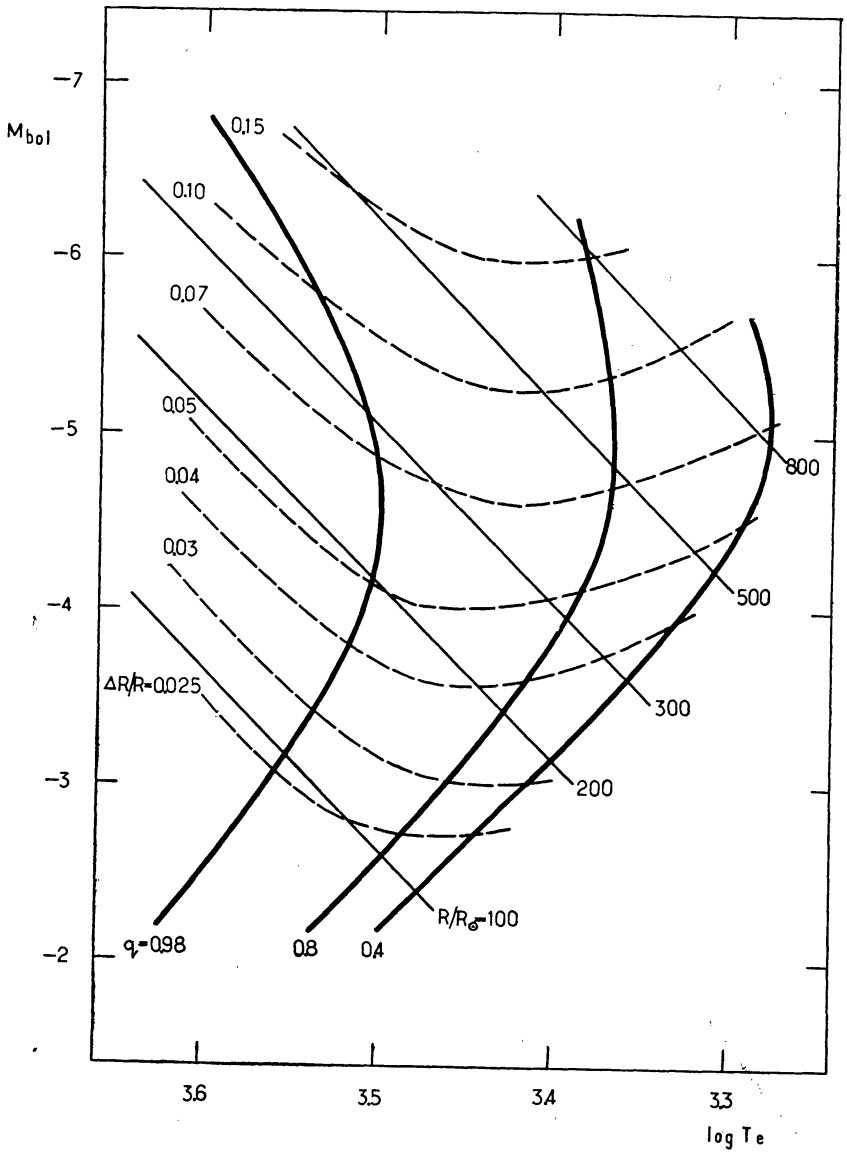

Fig. 6. The position of the model envelopes on the H—R diagram for a star of $1\,\mathfrak{M}_\odot$. Thick solid lines show the position of the models with a given fraction of mass q contained in the core. Thin solid lines are marked with the values of photospheric radii of the model envelopes. Broken lines are labelled with the values of fractional thickness of the model atmospheres, that is the thickness of layers with $0{\cdot}05 < \tau < 2/3$.

The fractional thickness of the atmospheres attached to our envelopes is shown in Fig. 6. This thickness may be as large as 15% of the photospheric radius for the most luminous models. The thickness of the atmosphere was measured by us as the distance between the layers at the optical depths 0·05 and 2/3. Auman (1968, Table IV)

© Copernicus Foundation for Polish Astronomy • Provided by the NASA Astrophysics Data System

1969AcA....19....1P

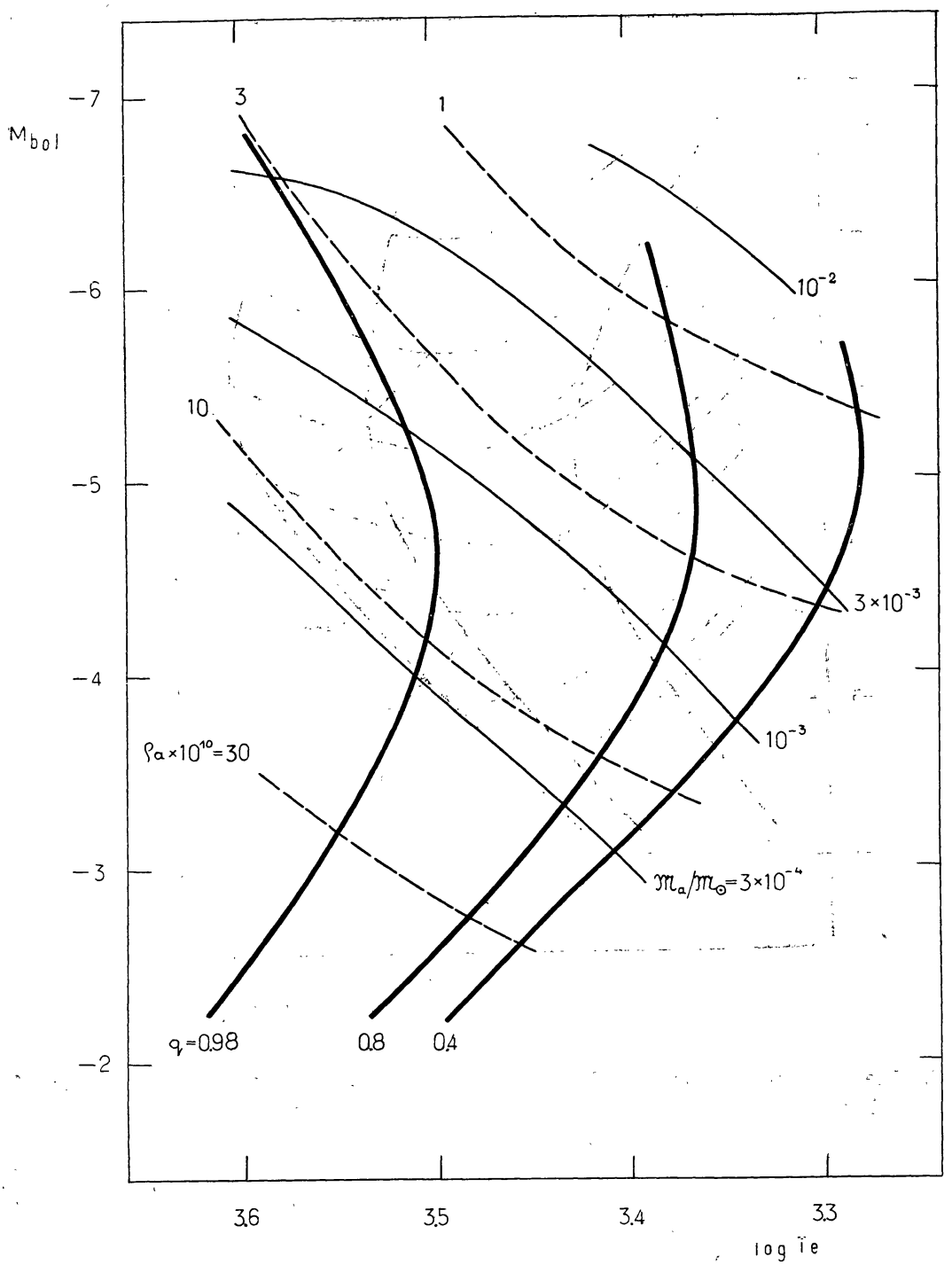

Fig. 7. The position of the model envelopes on the H—R diagram for a star of $1\,\mathfrak{M}_\odot$. Thick solid lines show the position of the models with a given fraction of mass q contained in the core. Thin solid lines are marked with the values of fractional mass of the model atmospheres, that is the mass above $\tau = 2/3$. Broken lines are labelled with the density of matter (in g/cm^3) in the photosphere, i. e. $\tau = 2/3$.

© Copernicus Foundation for Polish Astronomy • Provided by the NASA Astrophysics Data System

1969AcA....19....1P

also gives the fractional thickness of his model atmospheres of the red supergiants. Although our results cannot be directly compared, it seems that our models have thicker atmospheres than Auman's.

In the models with the photospheric temperature below 2600°K the convection was usually present in the atmosphere for the optical depths larger than 0·1 and smaller than about 2. It was due to the low value of the adiabatic gradient in the region where the H_2 molecules were partly dissociated. The velocity of the turbulent elements as computed from the mixing length theory was of the order of 20 meters per second and obviously had no influence on the structure of the atmosphere. The main convection zone usually appeared at the optical depth equal to 30. That convection carried a major part of the flux in the middle of a typical envelope, but the convective temperature gradient was always substantially larger than the adiabatic gradient similarly as in the envelopes studied by Paczyński and Ziółkowski (1968b).

The transition between the envelope and the core of the red supergiant is very rapid in the sense that the mass fraction of the transition region is very small. Therefore it is easy to define the mass of the core and of the envelope in a model of a whole star. Given the mass and the luminosity of the core, and the mass of the envelope, the model of the envelope is completly specified. It is well known that the evolution of a core of a supergiant star may be followed without detailed knowledge of the structure of the envelope. In this way Sugimoto and Yamamoto (1966) computed very advanced phases of evolution of a core of about 0·7 solar masses. The evolution of a star with total mass equal to 1 solar mass and a core like that studied by Sugimoto and Yamamoto may be followed on the H — R diagram with a help of our Figures 5 — 7 .

REFERENCES

Auman, J. Jr. . . . . 1967 *Ap. J. Suppl.*, **14**, 171.
. . . . . 1968 *Ap. J., in press.*

Auman, J. Jr., and Bodenheimer, P. . . . 1967 *Ap. J.*, **149**, 641.

Baker, N. H., and Temesváry, S. . . . . 1966 *Tables of Convective Stellar Envelope Models*, Goddard Space Flight Center, N. A. S. A.

Chandrasekhar, S. . . . . 1934 *M. N.*, **94**, 444.

© Copernicus Foundation for Polish Astronomy • Provided by the NASA Astrophysics Data System

1969AcA....19....1P

Henyey, L., Vardya, M. S., and Bodenheimer, P. . . . 1965 *Ap. J.*, **142**, 841.

Kamijo, F. . . . . 1968 *Z. f. Ap.*, **68**, 9.

Kippenhahn, R. . . . . 1963 *Proceedings of the International School of Physics „Enrico Fermi"*, **28**, 330.

Kosirev, N. A. . . . . 1934 *M. N.*, **94**, 430.

Paczyński, B. . . . . 1968 *Acta Astr.*, **18**, 511.

Paczyński, B., and Ziółkowski, J. . . . . 1968a *I. A. U. Symposium No.* **34***: „Planetary Nebulae"* (D. Reidel Pub. Co., Dordrecht), p. 396.

. . . . . 1968b *Acta Astr.*, **18**, 255.

Sugimoto, D., and Yamamoto, Y. . . . . 1966 *Prog. Theoret. Phys.*, **36**, 17.

Tsuji, T. . . . . 1964 *Ann. Tokyo Astr. Obs., Ser.* **2**, **9**, 1.

Vardya, M. S. . . . . 1960 *Ap. J. Suppl.*, **4**, 281.

Ziółkowski, J. . . . . 1968a *Astrophysics and Space Science, in press.*

. . . . . 1968b *Conference on the Mass Loss from the Stars*, Trieste.

Institute of Astronomy
Polish Academy of Sciences
Warsaw, September 1968

B. Paczyński

© Copernicus Foundation for Polish Astronomy • Provided by the NASA Astrophysics Data System